Hindawi
Modelling and Simulation in Engineering
Volume 2022, Article ID 1846193, 18 pages
https://doi.org/10.1155/2022/1846193

Research Article

Seismic Analysis on the Behaviors of *Meru* Structures: A Sacred Building in Balinese Temples

I Ketut Sudarsana,[1] **Gede Adi Susila**,[1] **Ni Putu Silvi**,[1] **and Ngakan Ketut Acwin Dwijendra**[2]

[1]*Department of Civil Engineering, Faculty of Engineering, Udayana University, Bali, Indonesia*
[2]*Department of Architecture, Faculty of Engineering, Udayana University, Bali, Indonesia*

Correspondence should be addressed to I Ketut Sudarsana; ksudarsana@unud.ac.id

Received 17 April 2022; Accepted 11 May 2022; Published 9 June 2022

Academic Editor: Nicolò Vaiana

Seismic behaviors of the *Meru* structure as one of the sacred buildings in Balinese Temples have not been investigated extensively. Most research investigated the Meru building in terms of its philosophy and history. The Meru buildings were observed to survive many earthquake events that occurred in Bali Islands. This paper presents the analysis results of the Meru structure in responding to earthquake excitations. As many as five types of the Meru structure traditionally built were modeled and analyzed using finite element-based software. Each type of Meru has three variations in the roof masses that were obtained from increasing the roof thickness from 500 mm, 600 mm, and 700 mm. Time history analysis follows Newmark's average acceleration method with an input earthquake record of the scaled El-Centro N-S 1940 to meet seismic conditions in the Bali area. The results show that the dynamic responses of the Meru structure increase as the number of roof levels and mass increase. All of the Meru types have met the limitation of the code's lateral allowable limits. The dimensions of the structural elements determined according to Balinese scripts can provide capacity greater than twice the capacity demand. Keeping the roof mass in a certain proportion with the mass of the lowest roof twice of the above one will keep the Meru stable during an earthquake.

1. Introduction

Meru is one of the sacred buildings in many temples in Bali as a landmark and symbol of the universe to worship gods and ancestors [1]. The shapes of Meru are high overlapping roofs as shown in Figure 1. The Meru structures are carefully designed, proportioned, and built according to *Asta Kosala Kosali* as local wisdom of Balinese traditional architecture by an *Undagi* (a Balinese craftsman) who has mastery in Balinese traditional architecture scripts. The Meru buildings were observed to survive many earthquake strikes in Bali Island. The Earthquake in 1815 and 1817 called *Gejer* Bali caused casualties of 10,253 people, and 1,500 people lost their lives in the Buleleng Earthquake in 1862, the Seririt Earthquake in 1976, and the Karangasem Earthquake in 2004. The earthquake sources outside Bali Island have also affected Bali such as Lombok Earthquake on August 5th, 2018, which destroyed many infrastructures in Bali. The earthquake resistance of the Meru buildings has been studied based on the architectural shape, meaning, and philosophy of the Meru building [1]. However, the Meru structure which is based on Balinese traditional architectures needs to be further studied against the earthquake loads although they were mostly found sturdy and stable during some past earthquake events that occurred in Bali. Research on the seismic behaviors of the Meru structures is not widely known; several studies on similar building shapes such as pagodas in Japan and China have been carried out.

Nakahara et al. [2] simulated earthquake resistance of Horyuji's five-story pagoda and showed the factors that help the structure to survive against earthquakes for almost 1300 years such as friction damping and sliding effect of the wooden joints, base isolation effects, balancing toy effects of deep eaves, and bolt fastening effect of the center column

Figure 1: The shape of Meru with high overlapping roofs.

[1]. Yuan and Li [3] summarized some research conducted by Chinese scientists on ancient pagodas in China that most materials used in the pagoda are wood with damping ratios ranging from 0.001 to 0.08. Most of the dynamic behavior of the pagoda was analyzed using a cantilever beam with continuous mass distribution or lamped mass distribution that resulted in the first mode of deformation which was bending deformation [3]. Kinematic Limit Analysis (KLA) and Dynamic Nonlinear Analysis (DNA) using pushover analysis were conducted by Endo and Hanazato [4] to study the dynamic behavior of the collapsed 5-tier pagoda in Nepal due to the Gurkha Earthquake in 2015. There were inconsistencies between the result of KLA and DNA with the damage to the pagoda during the earthquake due to some elements that have not been included in the modeling analysis. Song et al. [5] studied the behavior of a five-story timber pagoda in Shanghai during construction and found that the natural frequency of the pagoda during construction increases and then decreases after completion. The internal forces induced in the structural elements are about 6% of the elements' resistances. The infill wooden panel of mortise-tenon jointed frames used in the timber pagoda became shear resisting components and behaved nonlinearly with the ductility of 9.72 of the bare frames [6]. The building shape and structural materials of the Meru are similar to ancient wooden pagodas in China which consisted of two parts, namely, the lower structure from clay brick masonry as the base of the Meru and the upper structure from a wooden structure to support overlapping roofs. The base of the Meru symbolizes the earth [7]. The seismic behavior of the structure is affected by the total mass of the structure itself. In the Meru, the total mass is mainly due to the weight of the *Ijuk* as roof cover and also the total number of overlapping roofs. Since there was no study done to seek the effects of those parameters on the seismic behaviors of the Meru structure, the present analysis was carried out.

2. Analysis Procedures

2.1. Meru Structure. The Meru structure is built according to Balinese traditional architecture like other Balinese buildings which can be divided into three parts such as the head (roofs), body (worship place), and feet (base). The Meru plan is square having the size of the base varying from 3 m × 3 m, 5 m × 5 m, and 7 m × 7 m which is according to the number of overlapping roofs. The size of structural elements is calculated based on *Asta Kosala Kosali* (Balinese traditional architecture) which is three *guli* (=80 mm), three overlapping Balinese bundle coins (=90 mm), and *A rai* or *A musti* (=100 mm). The column sizes are proportioned to correspond to the number of overlapping roofs such as for the Meru with 3 and 5 overlapping roofs using the 1st column size of 80 mm, the Meru with 7 overlapping roofs using the 1st column size of 90 mm, the Meru with 9 and 11 overlapping roofs using the 1st column size of 90 mm, and the 2nd and 3rd column levels which are 80 mm. For other columns of all types, roof levels are proportioned to the size of the 1st column which is about 60 mm. The main beam size of the 1st level is 100 mm (*A guli* or *A musti*), and the next levels are proportioned to the beam size of the 1st level. Figure 2 shows plans and sections of the Meru having 3, 5, 7, 9, and 11 overlapping roofs. The structural details were drawn after consulting with a Meru craftsman (*Undagi*) in Gianyar Bali. Three sample connections of Meru's structural members are shown in Figure 3. Identifications of the outer and body columns in the Meru plan shown in Figure 2 are using red and blue colors, respectively.

2.2. Material Properties. The structure of Meru is usually built using *Cempaka* wood, the overlapping roof of *ijuk*, and red clay masonry bases. According to the Indonesian code for timber structure [8], the *Cempaka* wood has a volume weight ratio of 1000 kg/m^3, an elastic modulus of 8000 MPa (quality code E8), and a Poisson ratio of 0.18. The E8 quality code timbers have flexure, tension, compressive, shear, and compression perpendicular to the timber grin of 5.5 MPa, 4.9 MPa, 4.9 MPa, 0.65 MPa, and 1.3 MPa, respectively [8]. The material for the Meru roof cover is *ijuk* fibers having a volume weight ratio of 285 kg/m^3 for wet conditions [9]. The clay brick masonry base has a volume weight ratio of 1700 kg/m^3 and a modulus of elasticity of 240 MPa with a Poisson ratio of 0.15 [10].

2.3. Modeling and Structural Analysis. The seismic behavior analysis of the Meru was done using finite element-based program SAP2000 v.21. The structure was modeled 3-dimensionally (3D) where the structural elements such as beams, columns, and roof truss were modeled as frame elements. The Meru base of masonry clay bricks was modeled as solid elements. The *ijuk* roofs were modeled as shell elements with the roof thickness converted to be a gravity load acting downward. The traditional jointing system at the structural Meru uses wooden dowels as fixing elements, and they were assumed as semirigid connections with a rigidity factor of 0.2. The 1st column sits on a support element called *sendi* (*pin*) on the Meru base. The boundary conditions of the 1st column supports were modeled as a pin [11].

There were fifteen structural Meru models that were studied with variations in the number of overlapping roofs and the *ijuk* roof weight. The roof weights were calculated from the *ijuk* thickness, namely, 500 mm, 600 mm, and 700 mm.

The loads taken into account in the analysis were gravity, live, wind, and earthquake loads. The gravity loads are due to structural self-weight and the thickness of *ijuk* roofs

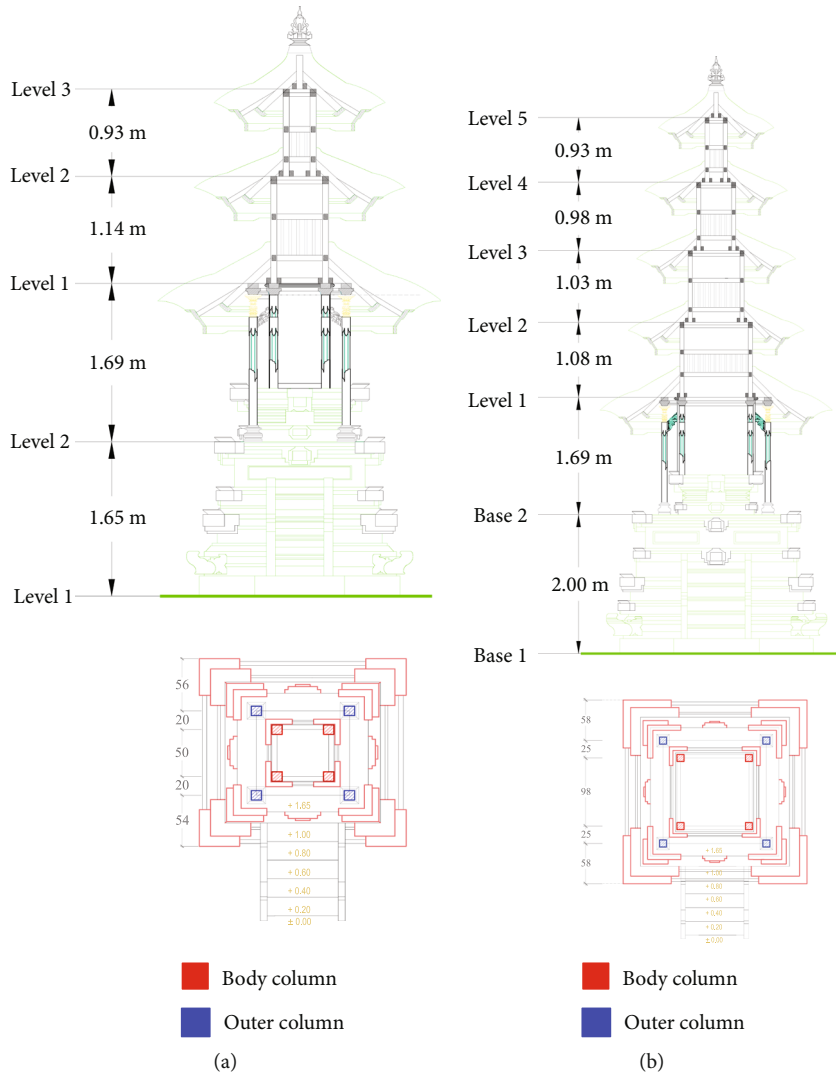

Figure 2: Continued.

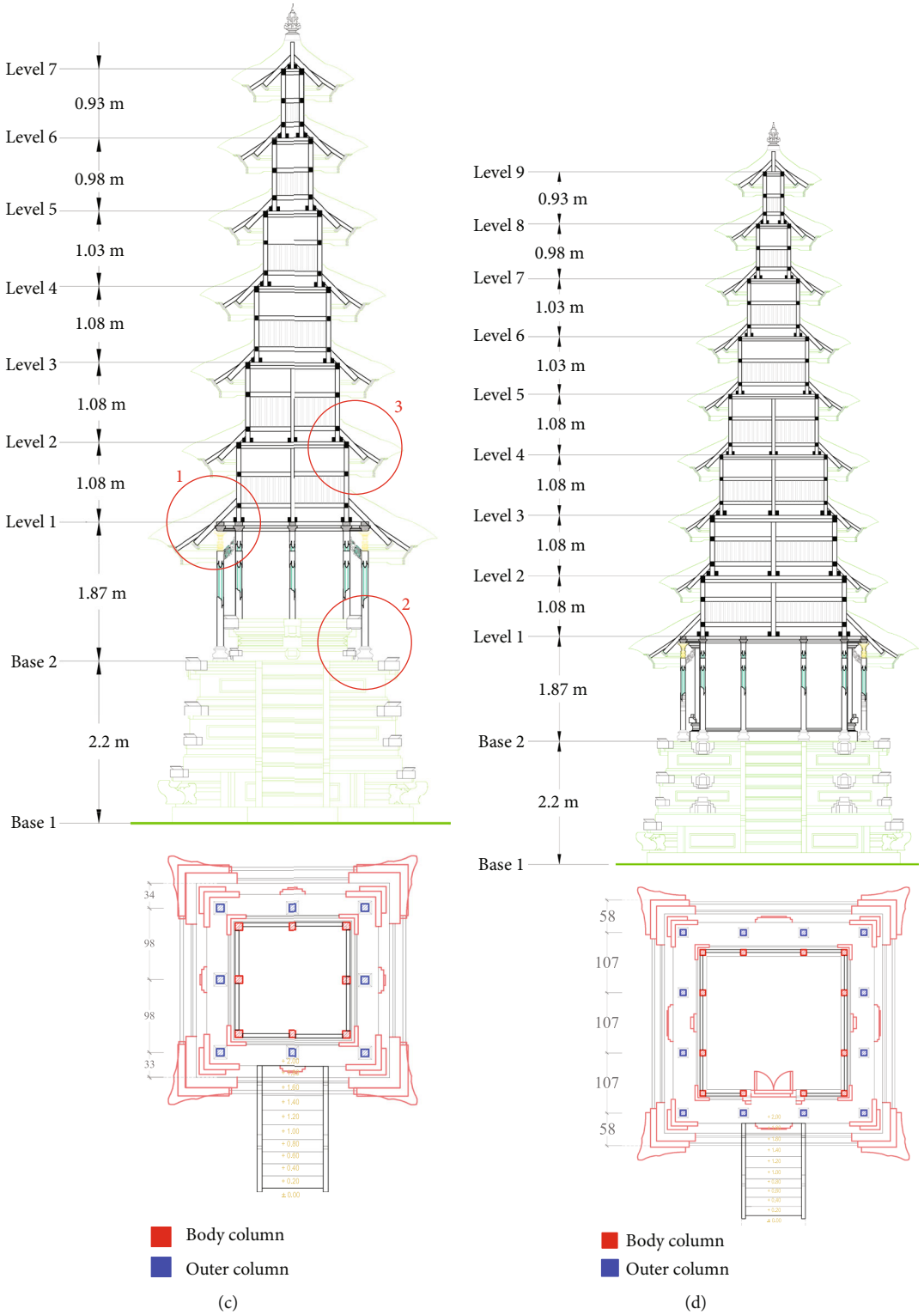

Figure 2: Continued.

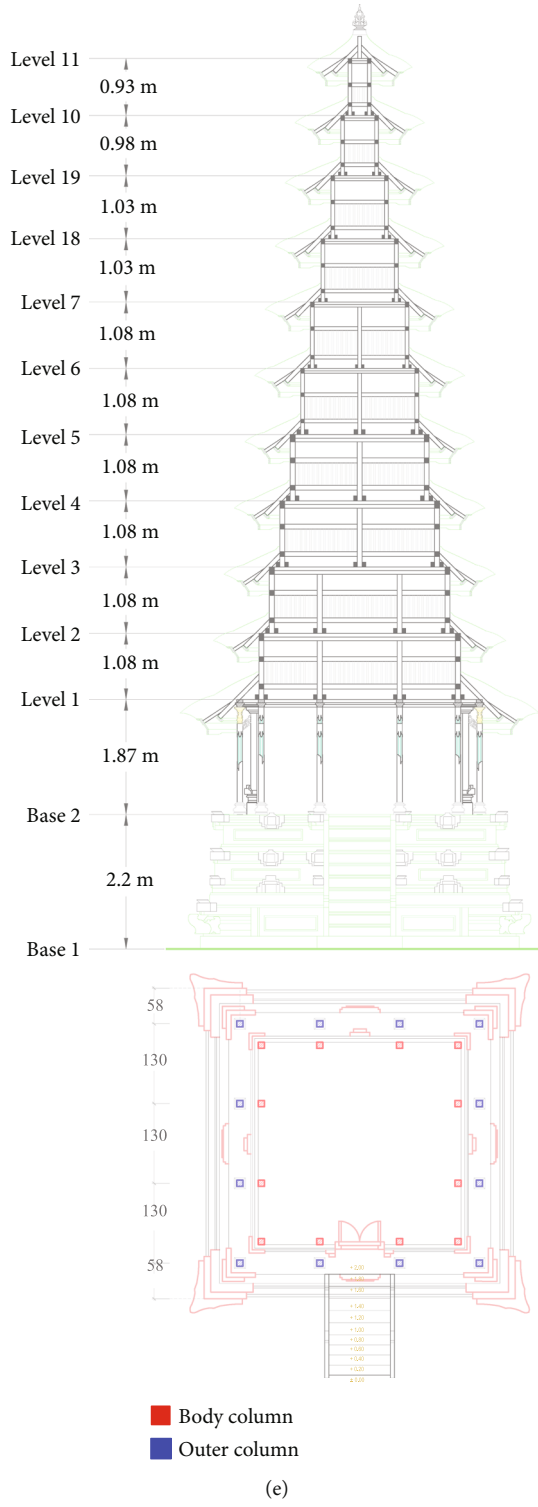

(e)

Figure 2: Plan and section of the Meru with 3, 5, 7, 9, and 11 overlapping roofs.

cover. The live load of 20 kg/m^2 was due to rainwater according to SNI 1727:2020 [12]. The wind loads were applied as autolateral loads of ASCE7-16 [13] with an adjusted parameter to meet the Indonesian code SNI 1727:2019. The characteristics of wind load were basic wind speed (v) of 70 km/hour or 43.5 mph with exposure category type B, topography (K_{zt}) of 1, wind blow effect factor (G) of 0.85, wind direction factor of 0.85, C_p windward of 0.7 and C_p Leeward of 0.4 [14], and wind direction angle of 0° and 90° to X and Y directions. The Meru structure is a timber cantilever truss as a seismic resisting force system with a seismic category of IV (monumental building) and an

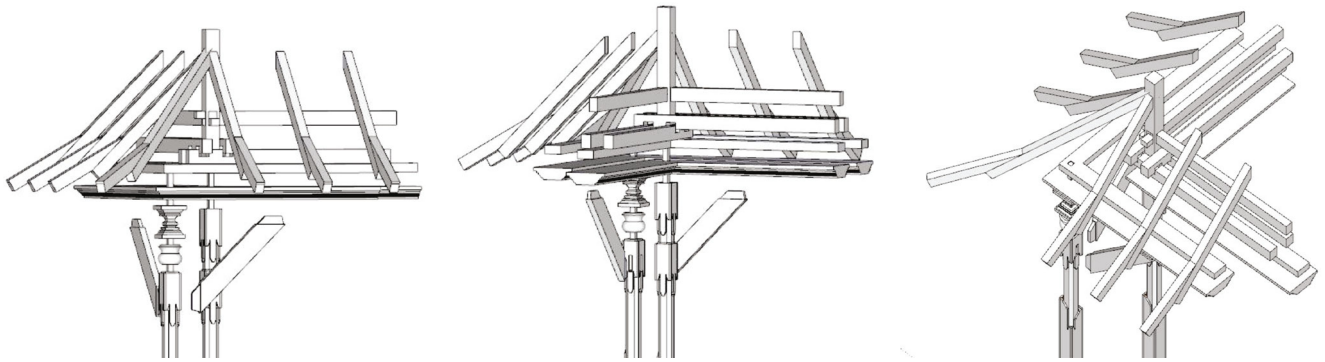

(a) Detail 1 (b) Detail 2 (c) Detail 3

Figure 3: Details of 3D connections as indicated in Figure 2(c).

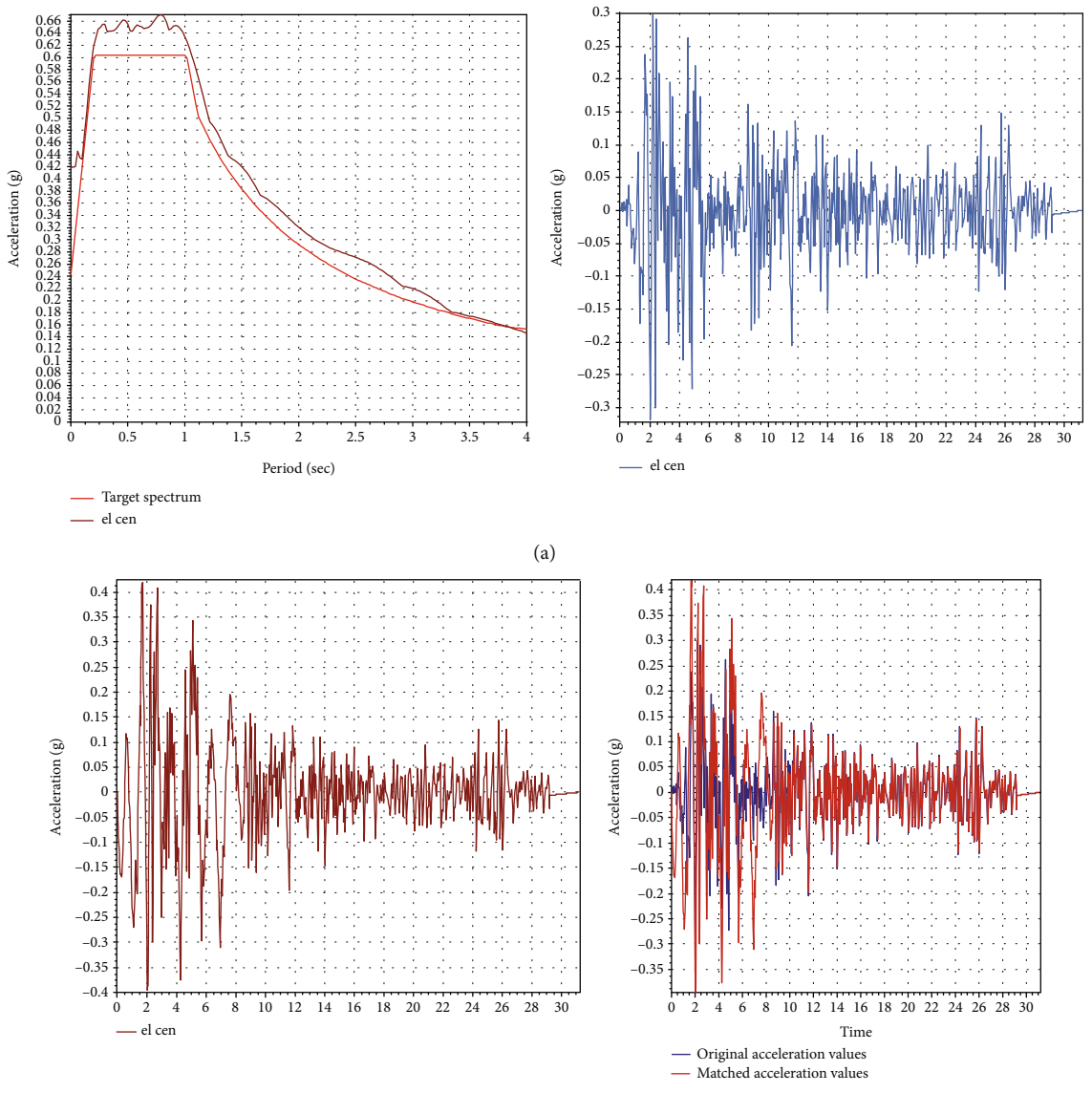

Figure 4: (a) *Matched accelerogram* El-Centro 1940 with spectrum response of Denpasar, (b) *original acceleration time history of El-Centro 1940 N-S*, and (c) *matched acceleration time history*.

Table 1: The fundamental period of several roof levels 3, 5, 7, 9, and 11.

Number of roof level	Model	Fundamental period (second)	h_n (m)	C_t	x	T_a	C_u	$T_a \cdot C_u$	Time period < $T_a \cdot C_u$
3	3a	0.222	5.41	0.0488	0.75	0.173	1.4	0.242	OK
	3b	0.233	5.41	0.0488	0.75	0.173	1.4	0.242	OK
	3c	0.242	5.41	0.0488	0.75	0.173	1.4	0.242	OK
5	5a	0.249	7.71	0.0488	0.75	0.226	1.4	0.316	OK
	5b	0.265	7.71	0.0488	0.75	0.226	1.4	0.316	OK
	5c	0.280	7.71	0.0488	0.75	0.226	1.4	0.316	OK
7	7a	0.320	10.21	0.0488	0.75	0.279	1.4	0.390	OK
	7b	0.340	10.21	0.0488	0.75	0.279	1.4	0.390	OK
	7c	0.359	10.21	0.0488	0.75	0.279	1.4	0.390	OK
9	9a	0.372	12.36	0.0488	0.75	0.322	1.4	0.450	OK
	9b	0.397	12.36	0.0488	0.75	0.322	1.4	0.450	OK
	9c	0.419	12.36	0.0488	0.75	0.322	1.4	0.450	OK
11	11a	0.421	14.52	0.0488	0.75	0.363	1.4	0.508	OK
	11b	0.448	14.52	0.0488	0.75	0.363	1.4	0.508	OK
	11c	0.473	14.52	0.0488	0.75	0.363	1.4	0.508	OK

important factor (I) of 1.5. Therefore, the value of response modification factor (R) of 1.5, overstrength factor (Ω_0) of 1.5, and lateral deformation amplification factor (C_d) of 1.5 taken from SNI 1726:2019 [15] was used in the seismic analysis. The model behaviors of the Meru were similar to that of Chinese timber pagodas [3].

The seismic load analysis was done using nonlinear direct integration time history following the average acceleration of Newmark's method by setting the value of $\gamma = 0.5$ and $\beta = 0.25$ [16] in which the method is unconditionally stable. In addition, Newmark's method is one of the most employed time integration methods available in the literature [17, 18]. The analysis considered the ground acceleration input using scaled El-Centro 1940 N-S record to meet the condition in Bali where SNI 1726:2019 defines the peak ground acceleration (PGA) of $0.3417g$ where g is an acceleration of gravity of $10\,\text{m/s}^2$. The PGA at the ground surface is affected by site class. The site class at Denpasar was soft soil and according to SNI 1726:2019, the PGA of $0.441g$, and giving the spectrum design in 0.2 seconds (S_{DS}) of $0.651g$ and the spectrum design for 1 second (S_{D1}) of $0.24g$. Since the value PGA of $0.441g$ is not shown in the SNI 1726:2019, it was interpolated linearly and obtained the value FPGA of 0.9. Then, the PGAM = FPGA × PGA = $0.9 \times 0.441g = 0.3969\,g$. Clause 11.1.4 of the SNI 1726:2019 describes that all ground acceleration used in the analysis shall be scaled to a ratio of I/R giving the PGAM of $\text{PGAM} \times (\text{I/R}) = 0.3969g \times (1.5/1.5) = 0.3969g$, and then, the scale factor was obtained to be $(0.3969/0.3417)\,g = 11.615\,\text{m/s}^2$, with the g value of $10\,\text{m/s}^2$. SeismoMatch 2018 software was used to scale the El-Centro 1940 accelerogram as shown in Figure 4.

3. Results and Discussion

3.1. Fundamental Periods. The fundamental period of a structure is important to determine the base shear of the structure induced by the earthquake using static analysis. The fundamental period is related to the 1st mode vibration of the structure in the translation's mode. The dynamic analysis results show that the vibration of the Meru structure is dominated by translation in the X and Y directions like the vibration of the cantilever beam. Table 1 shows the fundamental period of all types of the Meru model obtained from the analysis and compared with the Indonesian code requirements. The minimum (T_a) and maximum ($T_{\max}$) values of the fundamental period specified in SNI 1726:2019 [15] can be calculated using Equations (1) and (2), respectively,

$$T_a = C_t h_n^x, \tag{1}$$

$$T_{\max} = C_u T_a. \tag{2}$$

The parameters C_t, C_u, and x in Equations (1) and (2) are constant depending on the type of the structural system which are 0.0488, 1.4, and 0.75, respectively, for the Meru structure.

Table 1 shows that the fundamental period increases with the increase in the *ijuk* roof thickness with a nonproportional trend. Increasing the roof thickness by 100 mm gave the total mass of the structure increase by an average of 2.38% and resulted in the average increase of the fundamental period by 4.5%, 5.9%, 5.9%, 6.1%, and 6.1% for the Meru with the number of overlapping roof level of 3, 5, 7, 9, and 11, respectively. It was also found that increasing the number of overlapping roofs increases the fundamental period due to the mass and the stiffness increase; however, all of the Meru models exhibit a fundamental period less than the maximum values limited by SNI 1726:2019. It means that the proportion between the weight or mass and stiffness or height of the Meru structure is still acceptable.

3.2. Lateral Deformation. The lateral deformation of the Meru structure due to earthquake load in the X and Y

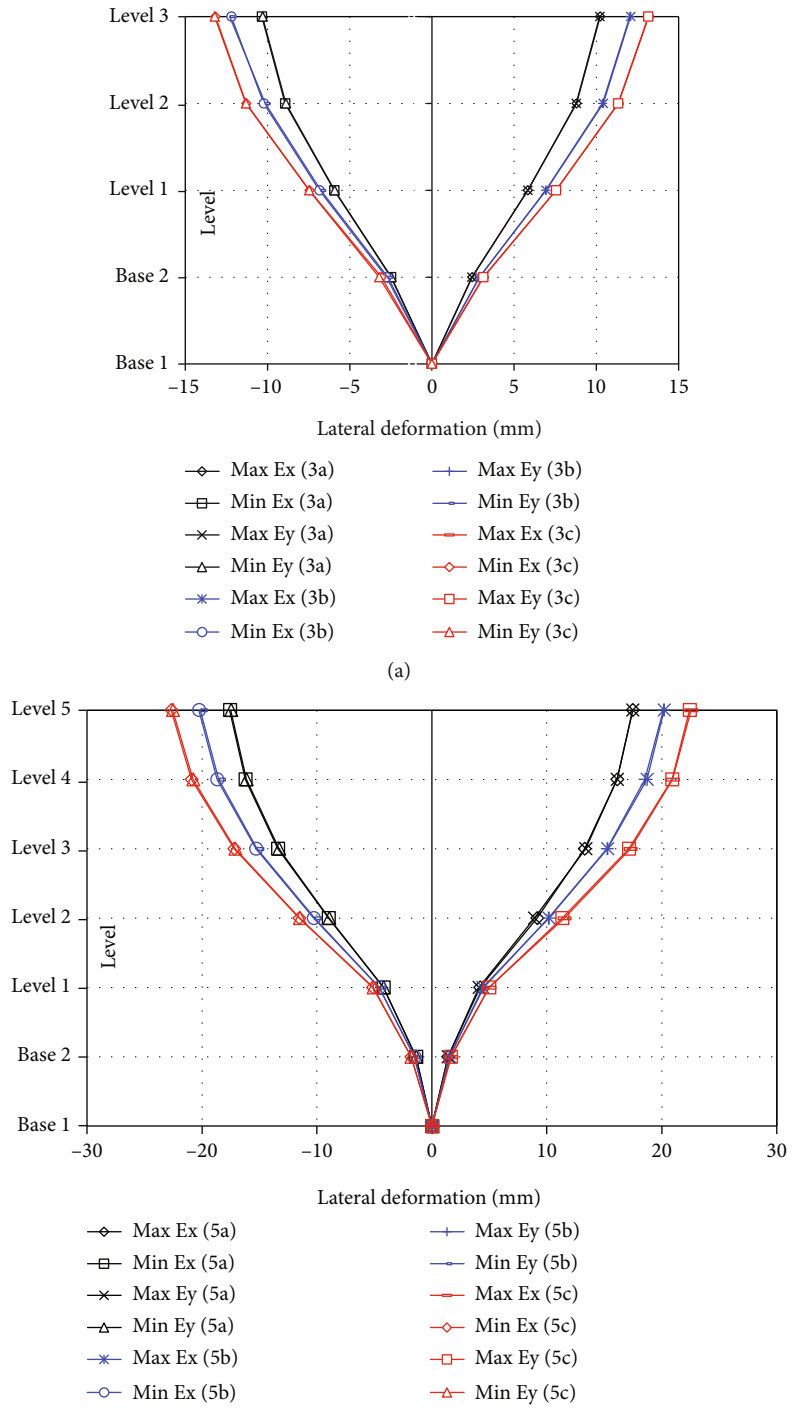

FIGURE 5: Lateral deformation due to the E_x and E_y Earthquake for Meru levels (a) 3 and (b) 5.

directions (E_x and E_y) can be seen in Figures 5–7. The maximum and minimum values of the lateral deformations differentiate the effect of the positive and negative values of the ground acceleration records. Figures 5–7 show that increasing the roof thickness hence the total mass of the Meru building results in an increase in lateral deformation for all types of the Meru. The maximum average increase in lateral deformation due to E_x and E_y is 11.89% ($E_{y\ \max}$), 11.39% ($E_{x\ \min}$), 11.66% ($E_{y\ \min}$), 12.40% ($E_{y\ \max}$), and 12.76% ($E_{x\ \min}$), respectively, for the number of roof levels 3, 5, 7, 9, and 11. The lateral deformations of all types of Meru are smaller than the allowable lateral deformation specified in SNI 1726:2019. The drift ratio is less than 130% indicating that all types of Meru structures do not experience a soft story mechanism.

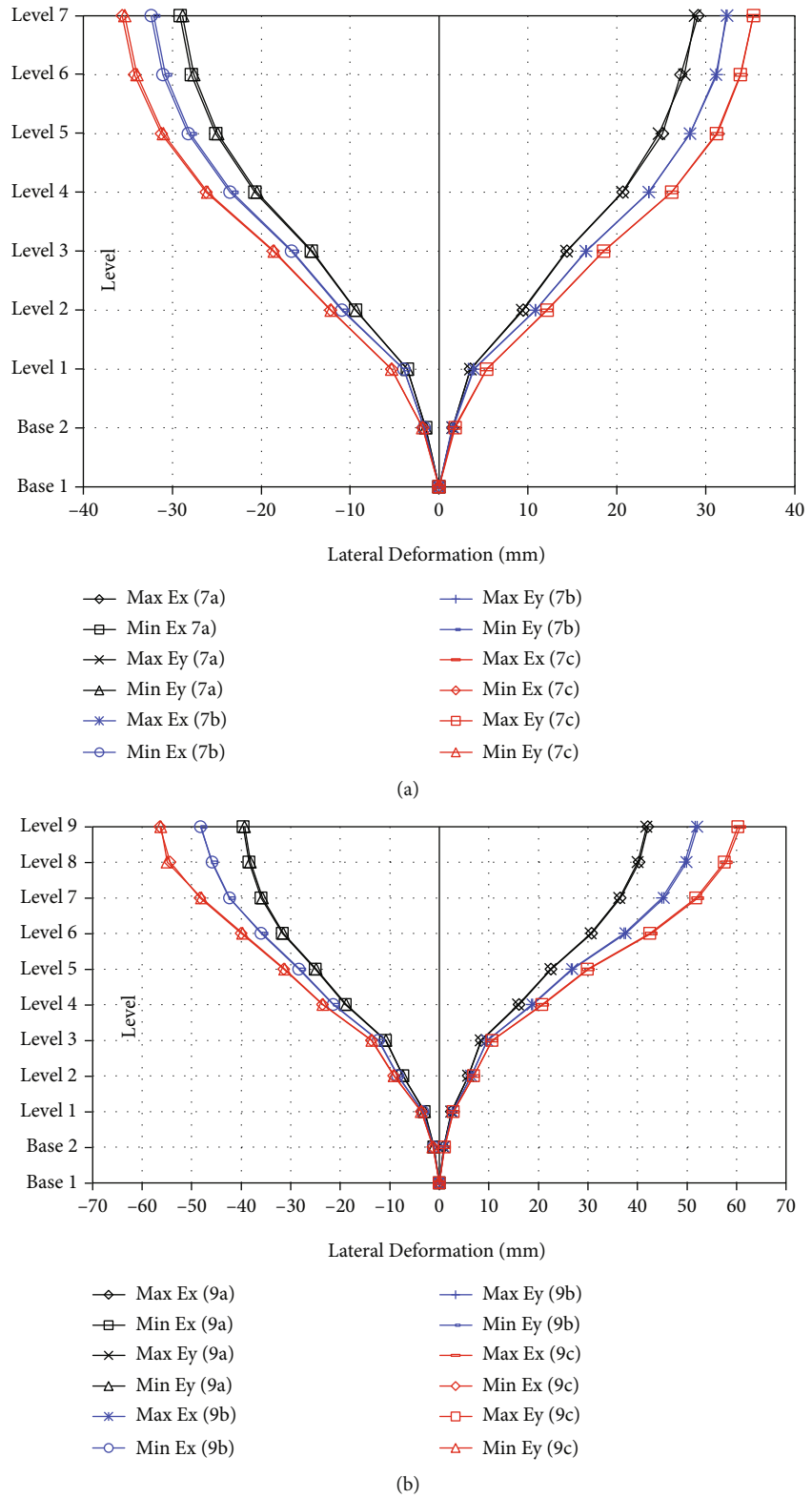

FIGURE 6: Lateral deformation due to the E_x and E_y Earthquake for Meru levels (a) 7 and (b) 9.

3.3. Base Shear (V_x and V_y). Earthquake load acts on the structure can be quantified as a base shear force which is proportional to the total mass of the structure and the acceleration of ground excitations. Table 2 shows the base shear of all types of the Meru and its percentage of the total mass. It is found that the percentage of base shear in X and Y directions to the total mass is similar about 46.40% to 50%. The percentage is not always affected by the number of

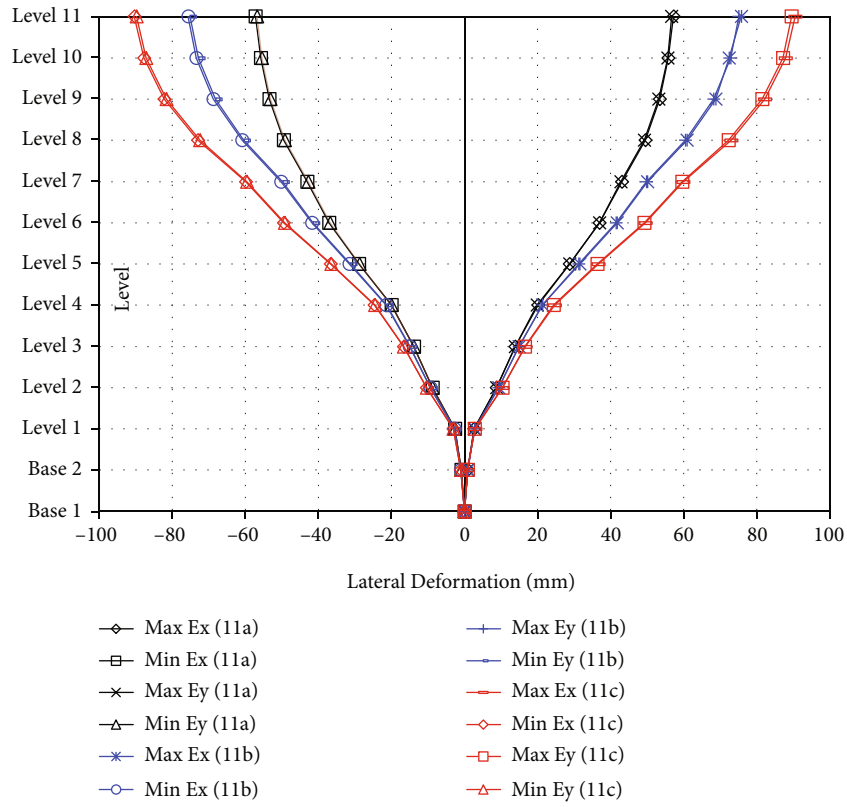

Figure 7: Lateral deformation due to the E_x and E_y Earthquake for Meru level 11.

Table 2: Base shear of Meru model due to the E_x and E_y Earthquake.

Number of roof level	Model	Total mass (kN)	Base shear in X and Y directions (V_x and V_y), in kilo Newton (kN)							
			V_x (max)	%Mass	V_x (min)	%Mass	V_y (max)	%Mass	V_y (min)	%Mass
3	3a	87.70	46.36	47.14%	-46.47	47.01%	46.33	47.14%	-46.49	46.99%
	3b	90.47	47.23	47.80%	-47.02	48.03%	47.20	47.80%	-47.05	48.00%
	3c	93.24	48.18	48.33%	-47.06	49.53%	48.13	48.33%	-47.08	49.51%
5	5a	234.48	116.72	50.22%	-125.66	46.41%	116.12	50.22%	-125.58	46.44%
	5b	239.83	118.79	50.47%	-127.17	46.98%	118.49	50.47%	-127.62	46.79%
	5c	245.19	120.64	50.80%	-129.60	47.14%	120.43	50.80%	-129.53	47.17%
7	7a	378.71	203.60	46.24%	-197.10	47.95%	203.31	46.24%	-197.18	47.93%
	7b	387.72	207.67	46.44%	-200.81	48.21%	207.27	46.44%	-200.84	48.20%
	7c	396.70	211.82	46.60%	-203.56	48.69%	211.32	46.60%	-203.51	48.70%
9	9a	777.31	418.00	46.23%	-400.43	48.49%	418.45	46.23%	-400.32	48.50%
	9b	794.81	423.13	46.76%	-404.93	49.05%	423.11	46.76%	-404.91	49.06%
	9c	812.31	424.15	47.78%	-412.93	49.17%	424.12	47.78%	-412.67	49.20%
11	11a	1080.44	550.77	49.02%	-549.77	49.12%	550.75	49.02%	-549.74	49.12%
	11b	1105.27	555.36	49.75%	-554.15	49.86%	555.13	49.75%	-554.12	49.87%
	11c	1130.07	559.09	50.53%	-558.56	50.57%	559.01	50.53%	-558.30	50.60%

overlapping roof levels. However, the base shear acting on the structure increases with the increase in the number of overlapping roofs as the total weight of the structure increases.

Table 2 shows that the greater the total mass of the building, the base shear due to the earthquake load in the X and Y directions increases with an average maximum increase of 1.91% ($V_{x,\max}$), 1.81% ($V_{y,\max}$), 1.96% ($V_{x,\max}$),

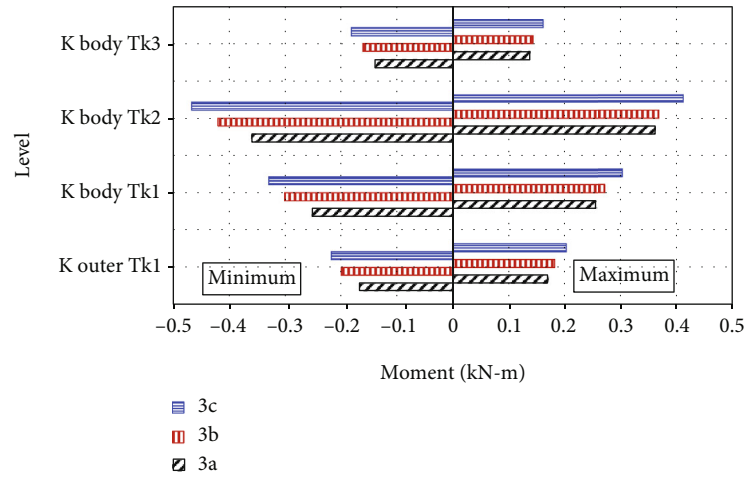

(a) Meru level 3

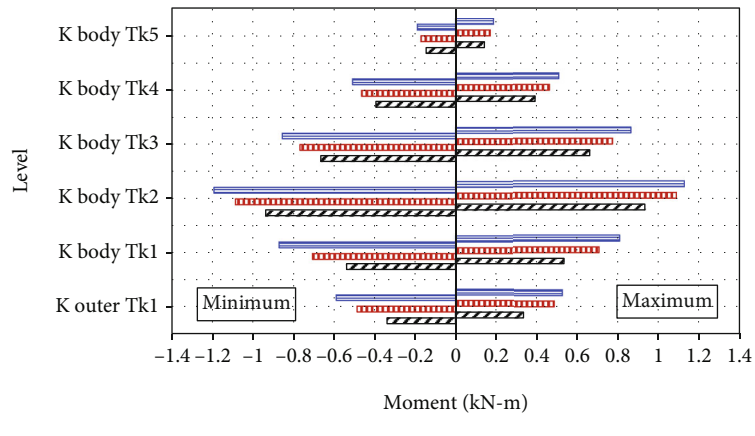

(b) Meru level 5

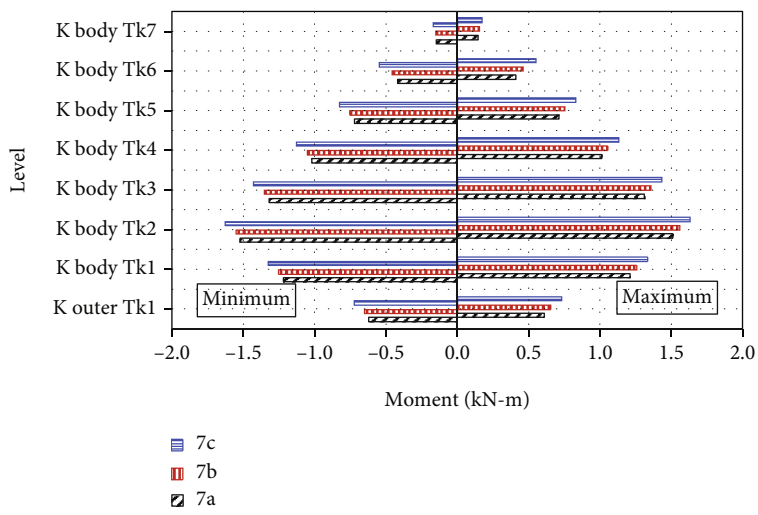

(c) Meru level 7

Figure 8: Continued.

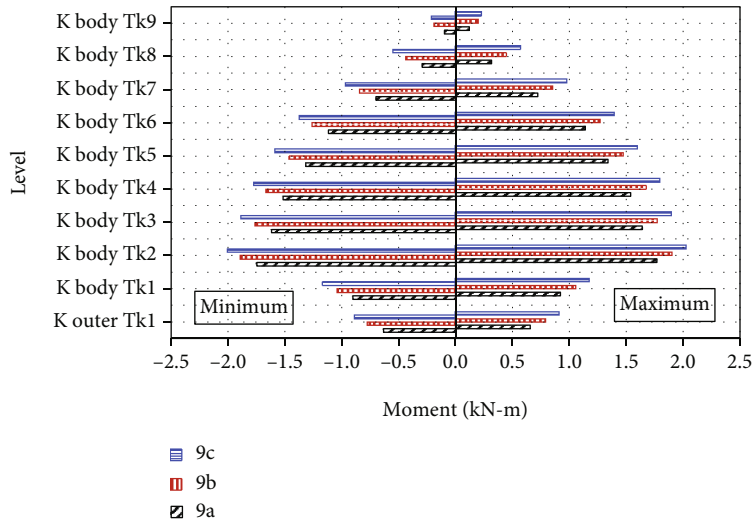

(d) Meru level 9

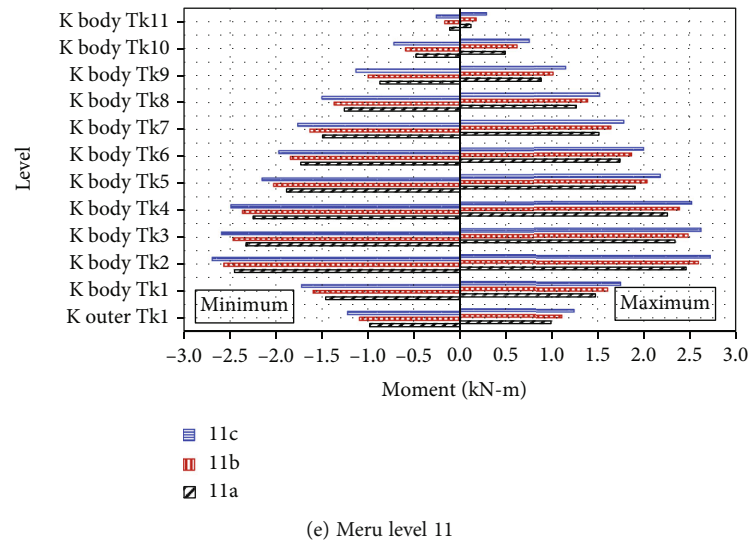

(e) Meru level 11

Figure 8: Column maximum moment due to earthquake load direction X for Meru levels 3, 5, 7, 9, and 11.

1.52% ($V_{x,\min}$), and 0.79% ($V_{x,\min}$) for the number of roof levels 3, 5, 7, 9, and 11, respectively. The higher the number of the Meru level, the base shear due to earthquake loads in X and Y directions increases with the maximum increase occurring for the $V_{y,\max}$ of 44.61%, 44.45%, and 44.34% for the *ijuk* thickness of 500 mm, 600 mm, and 700 mm, respectively.

3.4. Internal Forces at Structural Columns. The internal forces presented in this paper are only for the vertical elements or columns due to limited spaces, for internal forces of the other beams can be found in Silvi [19]. The columns were categorized into the outer columns for the 1st level only and the body columns at all levels as indicated in Figure 1. In addition, due to the symmetrical shape of the Meru building, only the internal forces due to an earthquake in X direction were presented.

Figures 8–10 show that the internal forces (axial, shear, and moment forces) of the columns for all types of the Meru structure increase from the top level to the 2nd level. The internal forces at the 1st level are divided into the internal forces of the body and outer columns. The higher internal forces have happened in the column at level 2. It is similar to the behavior of a cantilever column with a lumped mass at the roof level. Figures 8–10 also show that increasing the roof mass for each level on the average of 2.38% results in the maximum moments of the body columns due to the earthquake loads in X or Y directions increase by an average maximum of 12.34% ($E_{y\ \min}$), 14.00% ($E_{y\ \min}$), 5.67% ($E_{y\ \max}$), 13.92% ($E_{y\ \min}$), and 15.65% ($E_{y\ \min}$) for the number of roof levels 3, 5, 7, 9, and 11, respectively. The body column shear forces increase by an average maximum of 12.48% ($E_{y\ \max}$), 13.56% ($E_{y\ \min}$), 17.22% ($E_{y\ \min}$), 11.98% ($E_{y\ \max}$), and 5.57% ($E_{y\ \min}$), respectively, for the number of roof levels 3, 5, 7, 9,

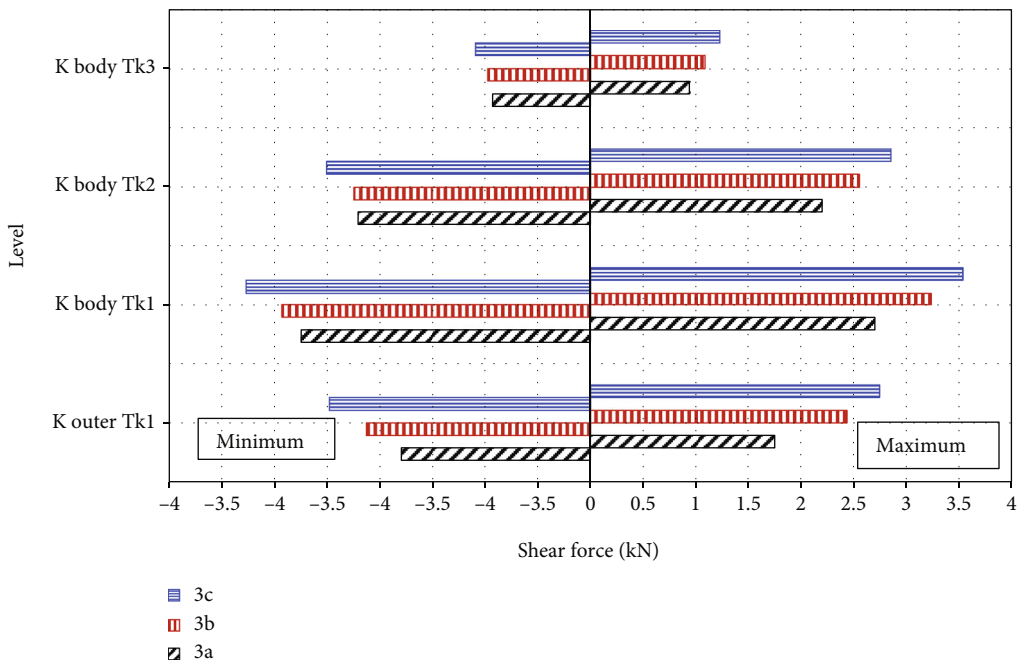

(a) Meru level 3

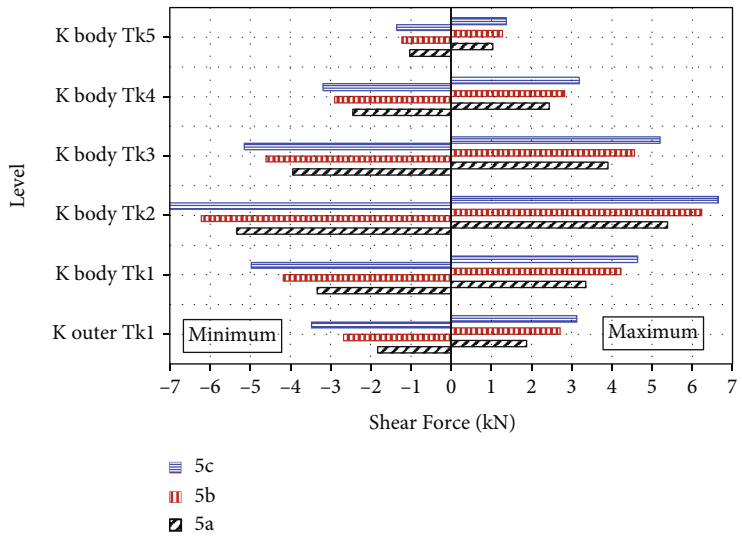

(b) Meru level 5

Figure 9: Continued.

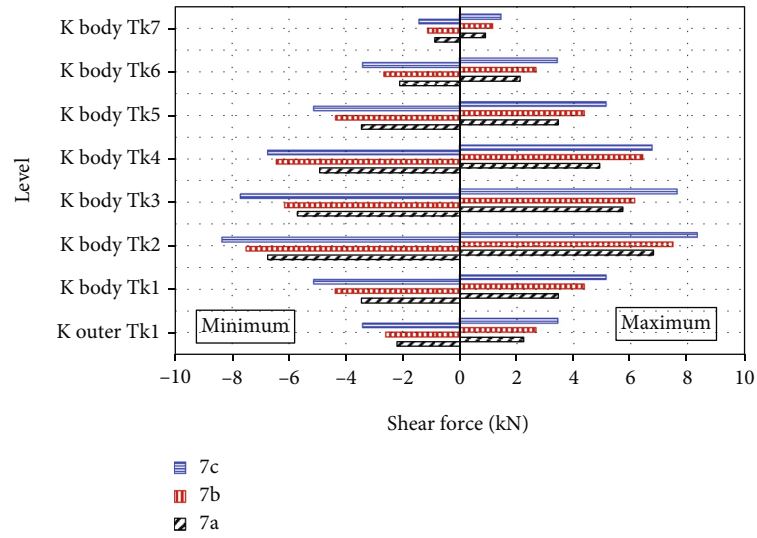

(c) Meru level 7

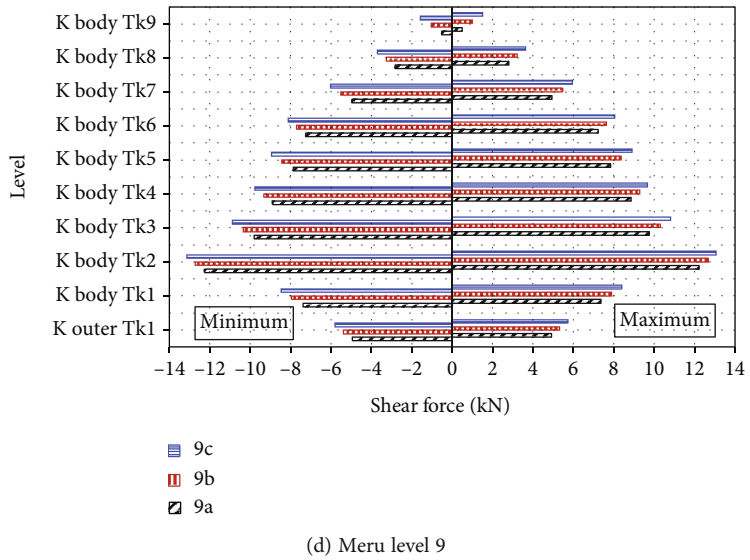

(d) Meru level 9

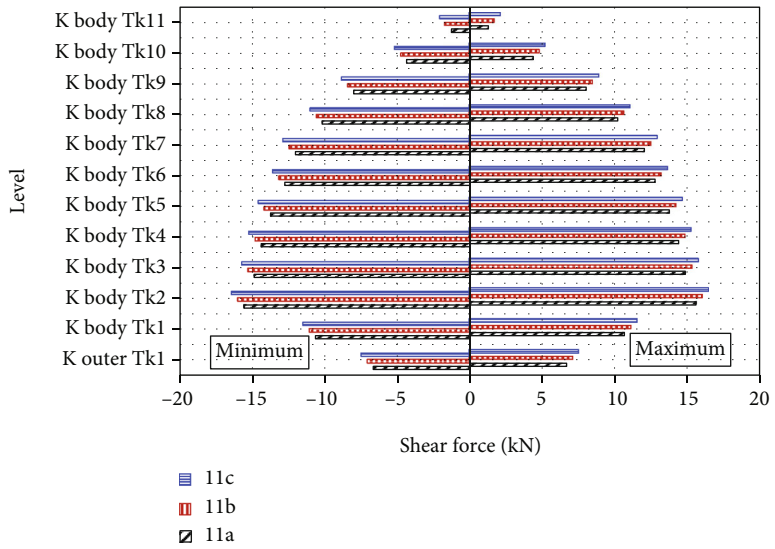

(e) Meru level 11

Figure 9: Column maximum shear force due to earthquake load direction X for Meru levels 3, 5, 7, 9, and 11.

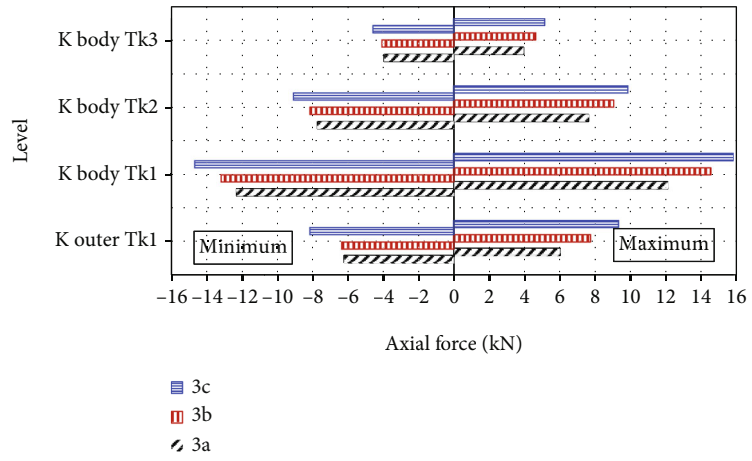

(a) For Meru level 3

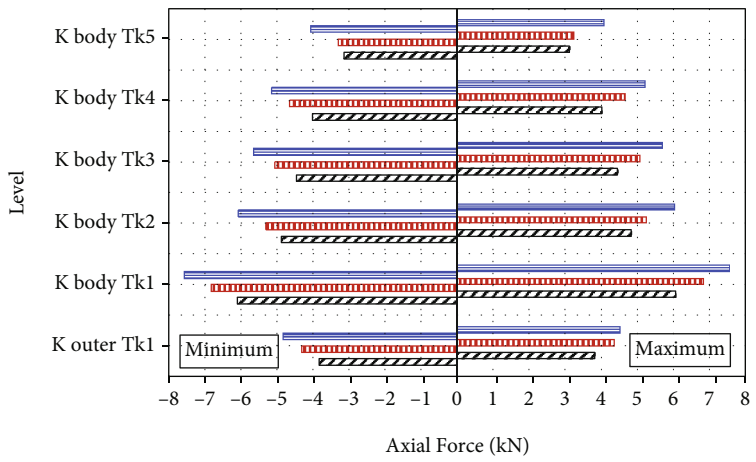

(b) Meru level 5

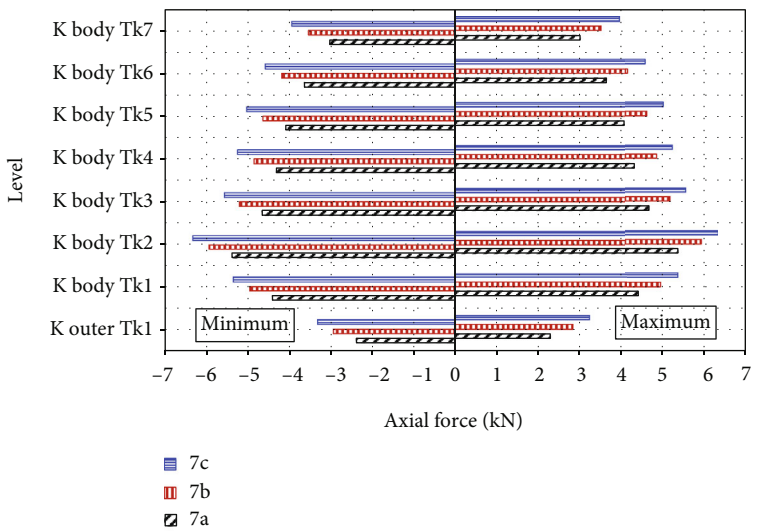

(c) Meru level 7

Figure 10: Continued.

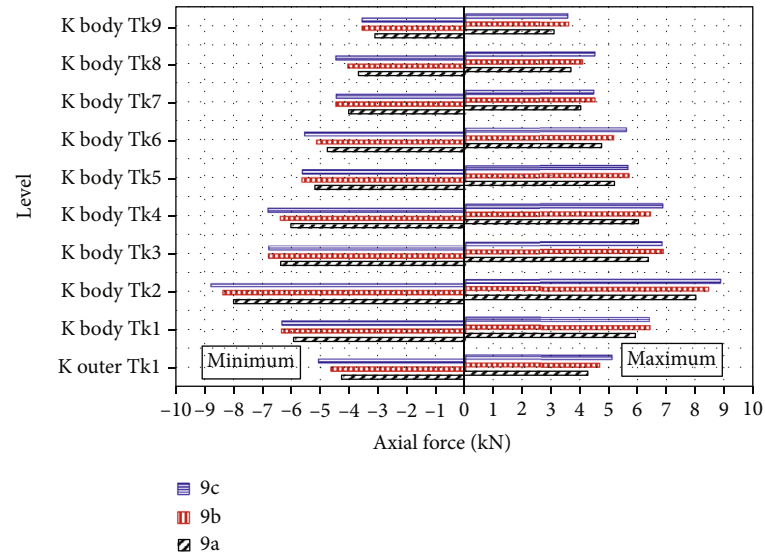

(d) Meru level 9

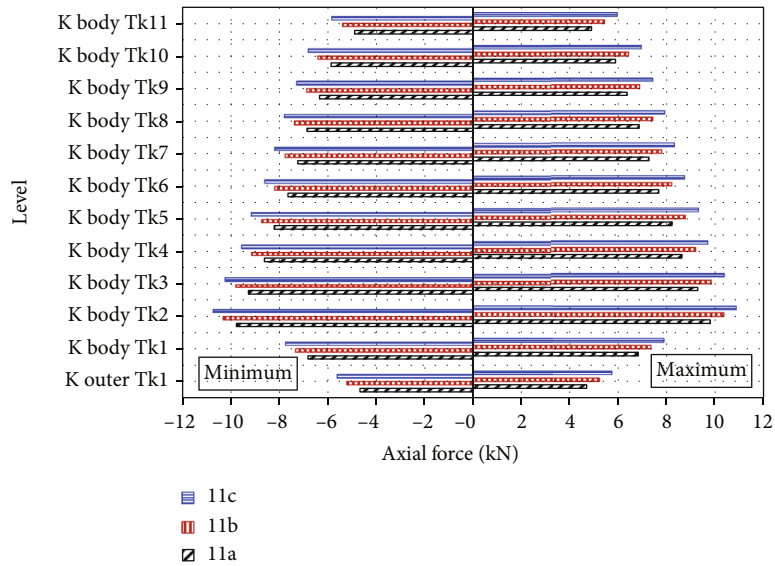

(e) Meru level 11

Figure 10: Column maximum axial force due to earthquake load direction X for Meru levels 3, 5, 7, 9, and 11.

and 11. The column axial forces also increase by an average maximum increase of 12.17% ($E_{y\ \min}$), 11.20% ($E_{y\ \max}$), 9.74% ($E_{y\ \max}$), 8.34% ($E_{y\ \min}$), and 6.65% ($E_{y\ \max}$) for the number of roof levels 3, 5, 7, 9, and 11, respectively.

The internal forces in the columns at the 1st level are supported proportionally by the body and the outer columns. The average ratios of the moment in the outer columns to that of the body columns for three different roof thicknesses or roof mass are 0.665, 0.656, 0.524, 0.744, and 0.693 for the number of levels 3, 5, 7, 9, and 11, respectively. The average ratios of shear forces are 0.726, 0.626, 0.644, 0.676, and 0.640 for number of levels 3, 5, 7, 9, and 11, respectively. The average ratios of axial forces are 0.539, 0.623, 0.565, 0.751, and 0.710 for number of levels 3, 5, 7, 9, and 11, respectively.

3.5. Design for Control Elements. The dimensions of the Meru structural elements (beams and columns) that are proportioned according to *Asta Kosala Kosali* (a Balinese traditional architecture script) were checked against the internal forces developed during the analysis. The load combinations considered in checking the elements' capacity were Comb5 $= 1.2D + E_x + 0.3E_y$, Comb6 $= 1.2D - 0.3E_x - E_y$, Comb7 $= 1.2D + 0.3E_x + E_y$, and Comb8 $= 1.2D - 0.3E_x - E_y$, where D is dead load due to the weight of the structure and roof cover (*ijuk*), E_x is earthquake load in the X direction, and E_y is earthquake loads in the Y direction. It was found that all beam and column dimensions specified according to *Asta Kosala Kosali* have met the requirements for strength and stability to resist the factored bending moments (M_u), shear (V_u), axial (P_u), and combination of axial and moments as

Table 3: Structural element design check for the number of roof levels 3 to 11.

Number of roof level	Variation roof thickness	Beam elements			Column elements		
		Avg. M_n/M_u	Avg. V_n/V_u	Avg. P_n/P_u	Avg. M_n/M_u	Avg. V_n/V_u	Max. stress ratio for comb. P_u and M_u (MPa)
3	3a	15.33	10.26	4.18	2.01	1.50	0.14
	3b	13.23	8.93	4.68	2.22	1.60	0.14
	3c	12.31	8.35	3.85	1.86	1.36	0.14
5	5a	14.10	19.91	3.86	4.08	3.02	0.08
	5b	12.72	18.16	3.44	3.61	2.69	0.09
	5c	11.32	16.63	3.14	3.33	2.50	0.10
7	7a	10.58	8.54	4.64	7.78	6.43	0.10
	7b	9.45	7.58	4.14	6.96	5.70	0.11
	7c	8.49	6.80	3.74	6.41	5.18	0.12
9	9a	12.50	7.87	3.71	4.51	2.58	0.09
	9b	7.99	7.11	3.26	4.02	2.32	0.10
	9c	7.44	6.83	2.94	3.70	2.14	0.11
11	11a	10.21	6.31	3.49	3.36	2.75	0.12
	11b	6.71	6.26	3.04	2.88	2.38	0.13
	11c	6.25	5.74	2.70	2.59	2.14	0.15

Table 4: *Ijuk* mass ratio of number of roof levels 3 to 11.

Roof level	The proportion ratio of *ijuk* roof mass for each level				
	Meru 3 levels	Meru 5 levels	Meru 7 levels	Meru 9 levels	Meru 11 levels
11	—	—	—	—	1.00
10	—	—	—	—	1.55
9	—	—	—	1.00	2.18
8	—	—	—	1.55	2.78
7	—	—	1.00	2.18	3.46
6	—	—	1.42	2.78	4.02
5	—	1.00	1.84	3.46	4.63
4	—	1.42	2.26	4.02	5.33
3	1.00	1.84	2.67	4.63	5.98
2	1.42	2.26	3.09	5.33	6.63
1	3.16	4.29	5.86	9.97	11.94

shown in Table 3. The average ratio of the element capacity to the capacity demand given in Table 3 indicates that the elements' capacities were much greater than factored load demands. The average values were taken among the size of beams and columns used in the structure for simplicity. The maximum stress ratios due to the combination of the factored bending moment and axial loads were far less than the stress specified in the code which is 0.65 MPa for the *Cempaka* timber.

3.6. Roof Mass Proportion. The mass of the *ijuk* fibers as a roof cover for each level is usually measured from the roof thicknesses. It may vary among the *Undagi* since there is no guidance for it. The Undagi usually installs the roof cover according to the overall looks of the Meru building. The analysis has been done on varying three different roof thicknesses hence the roof mass for each type of the Meru model and has found that by increasing the roof thickness up to 700 mm with a constant ratio among other levels, the structural elements were still safe and the whole structures were stable against lateral deformation due to earthquake loads. Table 4 shows the mass ratio of the *ijuk* roof for each type of Meru. In all Meru types, the biggest roof mass is at level 1 which is about twice the roof mass above it which can provide a balancing toy effect as in Chinese pagoda structures [3]. The least weight roof is at the top level which is about 42% of the roof's weight below it for the 3, 5, and 7 levels' Meru and about 55% for the 9

and 11 levels' Meru. This effect may contribute to the stable behavior of the Meru during earthquake events together with the structural system and materials of the Meru building.

4. Conclusion

Meru buildings are one of the sacred buildings found in many temples in Bali. As a sacred building located in a high seismic risk region, the behaviors of the Meru buildings against the earthquake loads need to be analyzed. Time history analyses have been conducted for fifteen structural models of Meru with variations on the number of overlapping roofs and thickness of the roof covers. The analysis results show that the natural period of the Meru structure increases as the total mass of Meru buildings increases. Increasing the mass of the overlapping roofs in each type of the Meru building results in an increase in the lateral deformation, maximum bending moments, shear, and axial forces of the body columns. The lateral deformation due to earthquake loads was less than the allowable lateral deformation specified in the SNI 1726:2019. The existence of the outer columns at the first level of all Meru reduced the internal forces supported by the body column at this level. The nominal capacities provided by the dimension of the structural elements obtained from the Balinese traditional architecture script (*Asta Kosala Kosali*) were much greater than the capacity demand due to factored internal force induced by the applied loads. To have a stable behavior of the Meru buildings, the weight proportion of the overlapping roofs within the Meru types must be kept proportional to other levels having the weight of the 1st level roof about twice the roof's weight above it and the top roof's weight about 42% to 55% less than the roof's weight below it.

Data Availability

The data used to support the findings of this study are available from the corresponding author upon request.

Conflicts of Interest

The authors declare that they have no conflicts of interest.

Acknowledgments

The study was sponsored by the Faculty of Engineering, Udayana University, Bali, Indonesia, which was greatly appreciated by the authors.

References

[1] N. K. A. Dwijendra, "Meru as a Hindu sacred building architecture with a high roof and resistant to earthquakes in Bali, Indonesia," *Indonesia*, vol. 8, no. 3, pp. 350–358, 2020.

[2] K. O. J. I. Nakahara, T. Hisatoku, T. Nagase, and Y. Takahashi, "Earthquake response of ancient five-story pagoda structure of Horyu-ji temple in Japan'," in *12th World Conference on Earthquake Engineering*, pp. 1–6, Japan, 2000.

[3] J. Yuan and S. Li, "Analysis and investigation of seismic behavior for multistory-pavilion ancient pagodas in China," *WIT Transactions on the Built Environment*, vol. 55, pp. 129–137, 2001.

[4] Y. Endo and T. Hanazato, "Seismic behaviour of a historic five-tiered pagoda in Nepal," *Structural Analysis of Historical Constructions*, vol. 18, pp. 1337–1345, 2019.

[5] X. Song, Y. Wu, K. Li et al., "Mechanical behavior of a Chinese traditional timber pagoda during construction," *Engineering Structures*, vol. 196, no. June, article 109302, 2019.

[6] E. Crayssac, X. Song, Y. Wu, and K. Li, "Lateral performance of mortise-tenon jointed traditional timber frames with wood panel infill," *Engineering Structures*, vol. 161, no. February, pp. 223–230, 2018.

[7] I. N. W. Paramadhyaksa, "Konsepsi Yang Melandasi Bagian Dasar Bangunan Meru di Bali," *Media Teknik*, vol. 3, pp. 229–238, 2008.

[8] SNI-7973, *Spesifikasi Desain untuk Konstruksi Kayu*, Badan Standarisasi Nasional, Jakarta, 2013.

[9] Supatmi, *Analisis Kualitas Genteng Beton dengan Bahan Tambah Serat Ijuk dan Pengurangan Pasir*, Universitas Negeri Yogyakarta, 2011.

[10] R. N. N. Rahayu, I. A. M. Budiwati, and M. Sukrawa, "Studi Karakteristik Bata MERAH Lokal Bali sebagai Dinding," *Jurnal Spektran*, vol. 4, no. 1, pp. 10–16, 2016.

[11] A. Awaludin and I. Irawati, *Konstruksi Kayu*, Biro Penerbit Teknik Sipil UGM, Yogyakarta, 2005.

[12] BSN SNI-1727, "Beban desain minimum dan Kriteria terkait untuk bangunan gedung dan struktur lain (SNI 1727:2020)," *Badan Standarisasi Nasional*, vol. 1727, no. 8, pp. 1–336, 2020.

[13] ASCE7-16, *Minimum design loads for buildings and other structures*, ANSI/ASCE Standard, 2000.

[14] G. A. Susila, "Wind load predicting; how could CFD replaced wind tunnel test," *Jurnal Ilmiah Teknik Sipil*, vol. 13, no. 1, 2009.

[15] BSN SNI-1726, "Tata Cara Perencanaan Ketahanan Gempa Untuk Struktur Bangunan Gedung dan Non Gedung (SNI 1726:2019)," *Sni*, vol. 1726, no. 8, p. 254, 2019.

[16] A. K. Chopra, *Dynamics of Structures: Theory and Aplications to Earthquake Engineering. Fourth*, Pearson Education Inc, New Jersey, USA, 2012.

[17] S.-Y. Chang, "Family of structure-dependent explicit methods for structural dynamics," *Journal of Engineering Mechanics*, vol. 140, no. 6, article 06014005, 2014.

[18] N. Vaiana, S. Sessa, F. Marmo, and L. Rosati, "Nonlinear dynamic analysis of hysteretic mechanical systems by combining a novel rate-independent model and an explicit time integration method," *Nonlinear Dynamics*, vol. 98, no. 4, pp. 2879–2901, 2019.

[19] N. P. Silvi, *Perilaku dinamis struktur meru [M.S. thesis]*, Program Studi Magister Teknik Sipil, Fakultas Teknik, Universitas Udayana, Denpasar, 2020.